High-energy Auger line shapes of Pd and Rh: Experiment and theory

G. G. Kleiman, R. Landers, S. G. C. de Castro, and A. de Siervo
Instituto de Física, ''Gleb Wataghin,'' Universidade Estadual de Campinas, 13081-970 Campinas, São Paulo, Brazil
(Received 29 June 1998; revised manuscript received 1 September 1998)

We compare nonrelativistic atomic multiplet calculations of the $L_{1,2,3}M_{4,5}M_{4,5}$ spectra of Rh and Pd in the *jj* intermediate-coupling scheme with high-resolution experimental spectra excited with a Ti anode, indicating general, good agreement even for these open valence shell metals: the simplicity of the calculations indicates their suitability for experimental analyses. Comparison with relativistic calculations, including configuration interaction, for Rh indicates that the nonrelativistic spectra appear to agree better with the experimental data than do the relativistic ones. The influence of relativistic and correlation effects on the intensities does not seem to be important. The major influence on the forms of the spectra is that of the relative positions of the multiplet components. Satellites of all three spectra would seem to be produced by shake-up, rather than Coster-Kronig processes. The positions and forms of these satellites are consistent with a model in which spectator vacancies in the $4d$ band exist in both the initial and final states of the Auger transition. [S0163-1829(98)02548-X]

I. INTRODUCTION

The use of x-ray excited Auger electron spectroscopy (XAES) as a tool for studying correlation effects in solid systems has been the subject of a great deal of research.[1–5] In studies of $3d$ and $4d$ metals, for many years, most attention was given to spectra with two final-state holes in the *d* band. In particular, the correlation between the final *d* holes was shown to be responsible for the quasiatomic forms of the $L_{2,3}M_{4,5}M_{4,5}$ spectra of Cu,[6,7] Zn,[7,8] Ge,[7,9] and Ga (Ref. 7) and of the $M_{4,5}N_{4,5}N_{4,5}$ of Ag, Cd, In, and Sm.[10]

In recent years, increasing attention has been given to high-resolution XAES of Auger transitions involving only core levels (i.e., *ijk* spectra), especially the $L_{2,3}M_{4,5}M_{4,5}$ spectra of the $4d$ metals,[11–32] for some of the following reasons: (i) comparison of experiment with atomic theory permits evaluation of the validity of the calculational schemes used and separation of atomic and solid-state effects, and (ii) predictions of Auger energies and theoretical expressions for Auger energy shifts should be compared to experimental quantities derived from *ijk* spectra. The core-level spectra have been measured in $4d$ metals whose *d* bands are full in the initial and final states of the Auger transition: that is, Ag (Refs. 11–16 and 20–29) and In, Sn, and Sb;[11,20,28,30] detailed comparisons of experimental and theoretical $L_{2,3}M_{4,5}M_{4,5}$ spectra have also been performed for these metals, giving satisfactory results.[11,23,30] Core-level spectra have also been measured in $4d$ metals whose *d* bands have holes: Pd,[14–17,19–22,25–29,31,32] Rh,[22,25,27,29,31,32] Ru,[25] and Mo and Nb.[20,21,25] For these metals, the only explicit atomic theoretical calculations were reported for Rh,[33] even though preliminary reports of comparisons of experimental and theoretical $L_{2,3}M_{4,5}M_{4,5}$ spectra were presented for Pd and Rh in another context.[31,32] The lack of reliable atomic theoretical spectral results for Pd has produced the peculiar situation that experimental $L_3M_{4,5}M_{4,5}$ spectra of Pd, taken with high-energy synchrotron radiation,[14,16,17,19] have been compared to atomic theoretical results for Rh.[33] The resulting good agreement is puzzling, in view of the difference in spin-orbit coupling between Pd and Rh.

In this paper, we report the results of *jj* intermediate-coupling atomic calculations of the $L_{1,2,3}M_{4,5}M_{4,5}$ spectra of Pd and Rh and compare them with the corresponding experimental high-resolution spectra, yielding generally good agreement for both metals. Comparison with relativistic intermediate-coupling computations from atomic theory, which include configuration interaction,[33] indicates that the present calculations, which are nonrelativistic, agree better with the Rh data than do the relativistic spectra, possibly because we have used x-ray photoemission spectroscopy (XPS) data to derive the spin-orbit coupling in our multiplet splittings. Inclusion of more sophisticated calculational effects, such as relativity and configuration interaction, appears to change the relative intensities of the atomic multiplet components too little to be experimentally observable. Furthermore, the results presented here permit simple calculations of the theoretical spectra, making them accessible to nontheorists. The experimental spectra presented here were excited with a Ti anode, which permits simultaneous measurement of all three $L_{1,2,3}M_{4,5}M_{4,5}$ spectra; these data were presented previously in a preliminary report.[29]

We describe the experimental details and the calculational procedure in Sec. II, discuss the results in Sec. III, and relate the conclusions in Sec. IV.

II. EXPERIMENTAL RESULTS AND CALCULATIONAL PROCEDURE

In previous studies,[20–28,31,32] we measured the high-energy L_2 and $L_3M_{4,5}M_{4,5}$ Auger spectra of Ag, Pd, and Rh using bremsstrahlung from an Al anode as the excitation source. Because of the desirability of recording the L_1, L_2, and $L_3M_{4,5}M_{4,5}$ spectra under the same conditions, for the present studies we used higher-energy exciting radiation from a Ti anode. The measurements reported here were performed using an ion-pumped system [base pressure of $(2-5)\times10^{-10}$ Torr] with a VSW HA 100 analyzer operated in the fixed analyzer transmission mode with a pass energy of 44.0 eV, which produces a full width at half maximum (FWHM) for the Au $4f_{7/2}$ line of 1.5 eV when excited by the

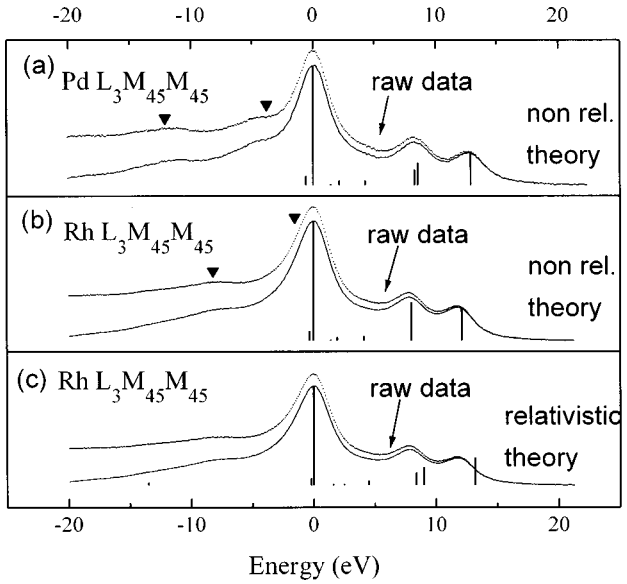

FIG. 1. $L_3M_{4,5}M_{4,5}$ Auger spectra of Pd and Rh as measured using a Ti anode (i.e., ''raw data'') and with background subtracted (Ref. 35). Energies are defined relative to those of the respective main (i.e., $^1G_4$) peaks, which are 2471.2 eV in Pd and 2360.8 eV in Rh. The downward solid triangles mark the positions of spectator vacancy satellites calculated from Eqs. (1) and (2). In (a), the bar diagrams represent the corresponding *jj* intermediate-coupling (IC) intensities from Table II. In (b), the Rh $L_3M_{4,5}M_{4,5}$ spectrum is compared to the nonrelativistic jj-IC intensities from Table I, while in (c) the same data are compared to the results of relativistic calculations (Ref. 33), given in parentheses in Table I.

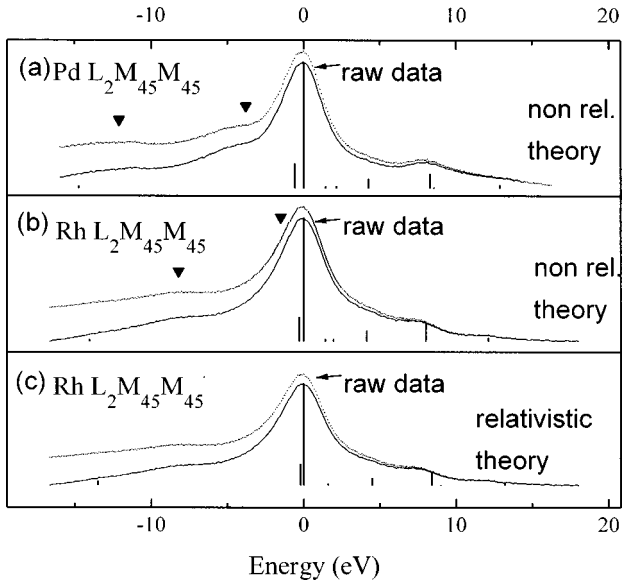

FIG. 2. $L_2M_{4,5}M_{4,5}$ Auger spectra of Pd and Rh with the same conventions as in Fig. 1. The energies of the respective main (i.e., $^1G_4$) peaks are 2628.6 eV in Pd and 2503.5 eV in Rh. The downward solid triangles mark the positions of spectator vacancy satellites calculated from Eqs. (1) and (2). In (a), the bar diagrams represent the corresponding *jj* intermediate-coupling (IC) intensities from Table II. In (b), the Rh $L_2M_{4,5}M_{4,5}$ spectrum is compared to the nonrelativistic jj-IC intensities from Table I, while in (c) the same data are compared to the results of relativistic calculations (Ref. 33) given in parentheses in Table I.

$K\alpha$ of Al. The $K\alpha_1$ ($\hbar\omega = 4510.9$ eV) and $K\alpha_2$ ($\hbar\omega = 4504.9$ eV) radiation from a Ti anode were employed to excite the Auger spectra and the energy scale was calibrated by measuring the Au $4f_{7/2}$ with Al $K\alpha$ and Ti $K\alpha_1$ radiation [binding energy 84.0 eV (Ref. 34)] and the Au *MNN* with the Ti $K\alpha_1$ line [2015.8 eV (Ref. 34)]. A detailed description of the sample preparation and experimental setup has already appeared in the literature.[20,21,28–30] The samples were in the form of thick high-purity foils polished to a mirror finish.

Because of the long acquisition times, all samples presented a slight oxygen contamination at the end of the analysis; the energies of the corresponding photoelectron peaks, however, were compatible with those of the clean pure metals.

In Figs. 1, 2, and 3, we present, respectively, the L_3, L_2, and $L_1M_{4,5}M_{4,5}$ spectra of Pd and Rh as functions of the kinetic energy relative to that of the main ($^1G_4$) peak. In each figure, we display the data before (designated as ''raw data'') and after subtracting a background calculated as a constant fraction of the experimental intensity integrated to higher kinetic energy than that considered.[35] In each figure, the Pd data are presented in panel (a) and the Rh data are presented in panels (b) and (c) in order to facilitate comparison with both our nonrelativistic calculations and the relativistic calculations of Chen.[33] The $L_1M_{4,5}M_{4,5}$ spectrum of Rh has been truncated at relative kinetic energies higher than 10 eV because of interference with the extraneous $L_2M_{4,5}N_{2,3}$ Auger spectrum at those energies. In each figure, we can separate the spectra into two regions: for positive relative energies, the spectra are dominated by atomic multiplets, and we denote this region as ''atomic;'' for negative relative energies, the structures can be identified with satellites. In previous work on the nature of these satellites[22,25,27,31,32] in Pd and Rh, we presented their $L_{2,3}M_{4,5}M_{4,5}$ spectra excited with bremsstrahlung. The use of a Ti anode improves the quality of these data and also permits measurement of good-quality $L_1M_{4,5}M_{4,5}$ spectra under the same conditions. The present data were presented previously in a preliminary study.[29]

The calculational procedure we use here is the same as that described in earlier work.[23,30] The equations we used for computing the theoretical $L_{2,3}M_{4,5}M_{4,5}$ spectra are those given in Ref. 30. Here, we present the equations for the $L_1M_{4,5}M_{4,5}$ transition probabilities, as well as other calculational details, in the Appendix. Briefly speaking, we calculated the relative energies of the final-state terms in the intermediate-coupling (IC) scheme[36] utilizing the atomic Coulomb integrals of Mann,[37] and the spin-orbit parameters used in the IC calculations were 2.11 and 1.90 eV for Pd and Rh, as derived from experimental $M_4 - M_5$ XPS splitting.[38] The results of our calculations of the multiplet energies, relative to that of the main ($^1G_4$) line, treating the final state in the IC scheme, are presented in the second columns of Tables I–III, along with the relativistic results of Chen for Rh[33] (in parentheses).

The transition rates were also calculated in the *jj* intermediate-coupling approximation, in which the initial state is treated in *jj* coupling and the final state in intermediate coupling, using the radial integrals calculated by McGuire.[39] The results for the $L_{1,2,3}M_{4,5}M_{4,5}$ IC transition rates relative to the most intense term are given for Rh and Pd in the third to fifth columns of Tables I and II, respec-

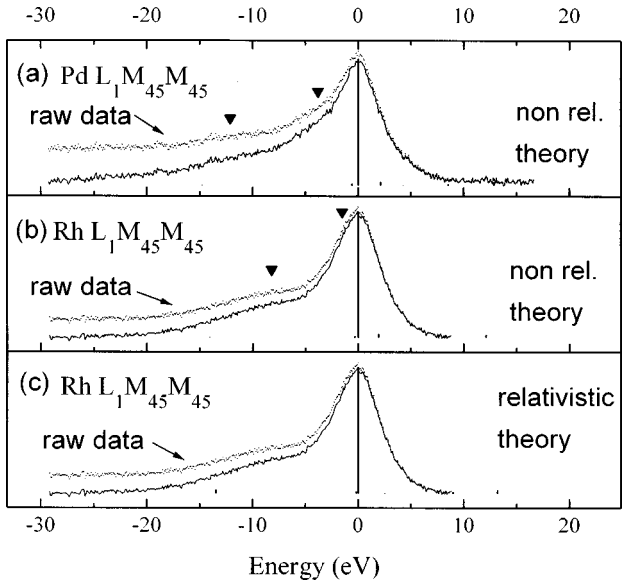

FIG. 3. $L_1M_{4,5}M_{4,5}$ Auger spectra of Pd and Rh with the same conventions as in Fig. 1. The energies of the respective main (i.e., $^1G_4$) peaks are 2902.6 eV in Pd and 2769.2 eV in Rh. The downward solid triangles mark the positions of spectator vacancy satellites calculated from Eqs. (1) and (2). In (a), the bar diagrams represent the corresponding *jj* intermediate-coupling (IC) intensities from Table II. In (b) and (c), the Rh $L_1M_{4,5}M_{4,5}$ spectrum is truncated at relative kinetic energies higher than 10 eV because of interference with the $L_2M_{4,5}N_{2,3}$ Auger. In (b), we present the nonrelativistic *jj*-IC intensities from Table I, while in (c) we exhibit the results of relativistic calculations (Ref. 33), given in parentheses in Table I.

TABLE I. Energies and intensities of the Rh $L_{1,2,3}M_{4,5}M_{4,5}$ spectra calculated in the *jj*-IC scheme relative to the respective $^1G_4$ terms. The order of the entries corresponds to that of the bars in Figs. 1–3. The indicated term is the zero spin-orbit limit of the IC state. The Rh energies and intensities in parentheses refer to the relativistic ones calculated by Chen in Ref. 33.

Term	Rel. energy	L_3MM Int.	L_2MM Int.	L_1MM Int.
$A\ (^1S_0)$	−14.03	0.032	0.034	0.025
	(−13.5)	(0.030)	(0.044)	(0.033)
$B\ (^3P_2)$	−0.30	0.074	0.191	0.013
	(−0.20)	(0.071)	(0.211)	(0.018)
$C\ (^1G_4)$	0.00	1.000	1.000	1.000
	(0.00)	(1.000)	(1.000)	(1.000)
$D\ (^3P_1)$	1.42	0.009	0.015	forbidden
	(1.60)	(0.012)	(0.020)	(0.000)
$E\ (^3P_0)$	1.96	0.010	0.001	0.003
	(2.50)	(0.014)	(0.001)	(0.004)
$F\ (^1D_2)$	4.14	0.040	0.087	0.001
	(4.50)	(0.048)	(0.075)	(0.001)
$G\ (^3F_3)$	8.01	0.131	0.126	forbidden
	(8.40)	(0.132)	(0.127)	(0.000)
$H\ (^3F_2)$	8.02	0.186	0.005	0.010
	(9.00)	(0.187)	(0.009)	(0.014)
$I\ (^3F_4)$	12.12	0.278	0.033	0.026
	(13.2)	(0.280)	(0.030)	(0.027)

TABLE II. Energies and intensities of the Pd $L_{1,2,3}M_{4,5}M_{4,5}$ spectra calculated in the *jj*-IC scheme relative to the respective $^1G_4$ terms. The order of the entries corresponds to that of the bars in Figs. 1–3. The indicated term is the zero spin-orbit limit of the IC state.

Term	Rel. energy	L_3MM Int.	L_2MM Int.	L_1MM Int.
$A\ (^1S_0)$	−14.74	0.025	0.034	0.031
$B\ (^3P_2)$	−0.58	0.073	0.196	0.013
$C\ (^1G_4)$	0.00	1.000	1.000	1.000
$D\ (^3P_1)$	1.44	0.010	0.016	forbidden
$E\ (^3P_0)$	2.15	0.011	0.001	0.004
$F\ (^1D_2)$	4.26	0.041	0.080	0.001
$G\ (^3F_3)$	8.28	0.132	0.126	forbidden
$H\ (^3F_2)$	8.54	0.186	0.006	0.011
$I\ (^3F_4)$	12.86	0.285	0.031	0.028

tively; the results of relativistic calculations for Rh (Ref. 33) are given in parentheses in Table I. Since the transition rates for the $L_1M_{4,5}M_{4,5}$ Auger process in Ag have never been published, we take this opportunity to present complete results for the $L_{1,2,3}M_{4,5}M_{4,5}$ transition rates and multiplet energies for Ag in Table III, correcting some typographical errors in Ref. 23. For our *jj*-IC calculations, the eigenvector mixing coefficients[36] corresponding to the entries in Tables I–III are those in Table IV. The equations used[40] are those given in Ref. 30 and in the Appendix of this paper.

The results of our calculations for Pd are represented by bars in Figs. 1(a), 2(a), and 3(a); those for Rh correspond to the bars in Figs. 1(b), 2(b), and 3(b); and the results of the relativistic calculations[33] for Rh are shown in Figs. 1(c), 2(c), and 3(c). The downward triangles in each panel correspond to the results of the calculations of the energies of shake-up satellites produced by spectator vacancies in the *d* band.[23]

For each metal, for negative relative energies, all three spectra exhibit satellites, whose forms are very similar for the L_2 and $L_3M_{4,5}M_{4,5}$ spectra, although somewhat broader for the $L_1M_{4,5}M_{4,5}$ spectrum.

III. DISCUSSION

The points we wish to discuss, when comparing our nonrelativistic calculations with those including relativistic ef-

TABLE III. Energies and intensities of the Ag $L_{1,2,3}M_{4,5}M_{4,5}$ spectra calculated in the *jj*-IC scheme relative to the respective $^1G_4$ terms. The order of the entries corresponds to that of the bars in Figs. 1–3. The indicated term is the zero spin-orbit limit of the IC state.

Term	Rel. energy	L_3MM Int.	L_2MM Int.	L_1MM Int.
$A\ (^1S_0)$	−15.57	0.023	0.034	0.031
$B\ (^3P_2)$	−1.04	0.071	0.202	0.013
$C\ (^1G_4)$	0.00	1.000	1.000	1.000
$D\ (^3P_1)$	1.45	0.010	0.016	forbidden
$E\ (^3P_0)$	2.44	0.011	0.000	0.004
$F\ (^1D_2)$	4.35	0.045	0.071	0.000
$G\ (^3F_3)$	8.54	0.132	0.125	forbidden
$H\ (^3F_2)$	9.22	0.186	0.008	0.011
$I\ (^3F_4)$	13.77	0.294	0.027	0.033

TABLE IV. Eigenvectors for $4d^8$ states in intermediate coupling (J,i). The second column indicates the zero spin-orbit coupling limit of state (J,i). The eigenstates are presented in the same order as the lines in the figures.

$C_{Ji}(^{2S+1}L_J)$	Zero spin-orbit limit	Rh	Pd	Ag
$C_{0A}(^1S_0)$	$^1S_0$	0.9521	0.9463	0.9374
$C_{0A}(^3P_0)$		0.3056	0.3232	0.3483
$C_{2B}(^1D_2)$	$^3P_2$	0.7311	0.7303	0.7272
$C_{2B}(^3P_2)$		−0.5569	−0.5399	−0.5165
$C_{2B}(^3F_2)$		0.3941	0.4185	0.4521
$C_{4C}(^1G_4)$	$^1G_4$	−0.9873	0.9861	0.9842
$C_{4C}(^3F_4)$		0.1588	0.1664	0.1771
$C_{1D}(^3P_1)$	$^3P_1$	1.00	1.00	1.00
$C_{0E}(^1S_0)$	$^3P_0$	0.3056	0.3232	0.3484
$C_{0E}(^3P_0)$		−0.9521	−0.9463	−0.9374
$C_{2F}(^1D_2)$	$^1D_2$	0.2210	0.1713	0.1054
$C_{2F}(^3P_2)$		0.7398	0.7378	0.7348
$C_{2F}(^3F_2)$		0.6354	0.6529	0.6700
$C_{3G}(^3F_3)$	$^3F_3$	1.00	1.00	1.00
$C_{2H}(^1D_2)$	$^3F_2$	0.6454	0.6613	0.6783
$C_{2H}(^3P_2)$		0.3775	0.4051	0.4396
$C_{2H}(^3F_2)$		−0.6640	−0.6314	−0.5888
$C_{4I}(^1G_4)$	$^3F_4$	0.1588	0.1664	0.1771
$C_{4I}(^3F_4)$		0.9873	0.9861	0.9842

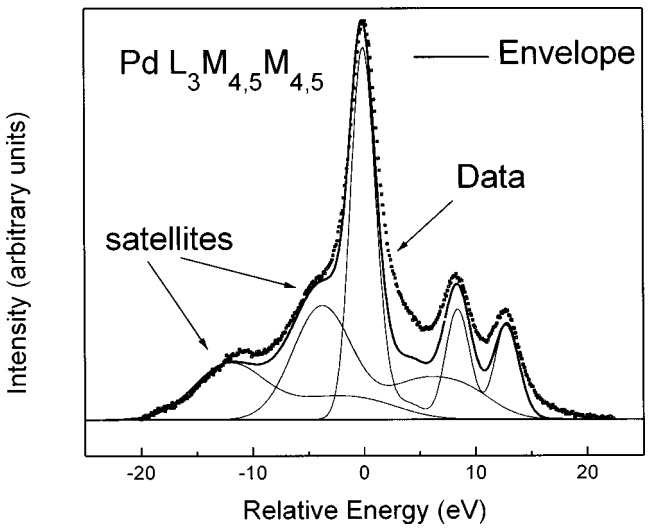

FIG. 4. $L_3M_{4,5}M_{4,5}$ spectrum of Pd with background removed (Ref. 35) as a function of energy relative to that of the $^1G_4$ peak (i.e., 2471.19 eV). The data are compared to an envelope of the nonrelativistic theoretical atomic multiplet spectrum and two satellite ''image'' spectra, which are broadened versions of the atomic spectrum. The atomic spectrum was calculated by associating Gaussians of constant width and amplitude with each multiplet component. The parameters used in the calculations are given in Table V. The relative positions of the $^1G_4$ peaks of the images are calculated from Eq. (1) for the closer satellite and Eq. (2) for the further satellite.

fects and configuration interaction,[33] are most readily illustrated by the Rh $L_3M_{4,5}M_{4,5}$ Auger spectra, in Figs. 1(b) and 1(c), since the other Rh spectra become progressively more featureless. It is surprising to note that the nonrelativistic calculational results seem to agree better with experiment than do those of the relativistic calculations.[33] This impression is less easy to sustain for the other Rh Auger spectra in Figs. 2 and 3, since the featureless nature of the spectra impedes drawing definitive conclusions. Another surprise, when inspecting Table I, is that the relative intensities of both calculations agree rather well; calculations of Rh $L_{2,3}M_{2,3}M_{4,5}$ theoretical spectra indicate a difference of as much as 10% between the nonrelativistic[41] and the relativistic[33] relative intensity results. What accounts for the difference between Figs. 1(b) and 1(c) is in the calculation of the multiplet energies.

Our calculation utilizes experimentally derived spin-orbit coupling, whereas the relativistic calculation yields the values of the multiplet splittings. It is difficult to pinpoint the roots of the discrepancy for Rh noted in Fig. 1 because of the various approximations made in the relativistic calculation[33] and because of its complexity. The Coulomb integrals (F^2 and F^4 in the notation of Slater[42]) we use are derived from a self-consistent neutral ground-state Hartree-Fock-Slater calculation (HF-SCF),[37] with exact treatment of exchange. In the relativistic calculations,[33] the Slater integrals were apparently[43] computed from Dirac-Hartree-Slater (DHS) for the initial Auger state, with one L hole. Increasing our F^2 and F^4 values by 10%, while keeping their ratio constant,[44] in order to simulate the effect of including hole states in the basis functions (instead of the neutral ground state),[44] produces a multiplet splitting similar, but not identical, to that resulting from the relativistic calculation.[33] Furthermore, the relativistic calculation for Rh has been used to describe the Pd $L_3M_{4,5}M_{4,5}$ Auger spectrum:[14,16,17,19] comparing the nonrelativistic Pd and relativistic Rh results in Tables I–III indicates considerable resemblance.

In the language of our calculation, then, the relativistic results appear to correspond roughly to Coulomb interactions in the presence of an increased nuclear charge. The question then is why the ground state would be appropriate for determining the final-state hole interaction, which determines the multiplet splittings. The discrepancy for Rh would then be attributable to overestimating the Coulomb interaction between the final-state holes in the relativistic calculation,[33] relativistic corrections would seem to have little effect on the multiplet splitting. A possible answer to the question might involve the neglect of valence *d*-electron screening in the relativistic atomic calculations for Rh.[33] Such an explanation, however, would not be consistent with the good agreement between our calculations and experiment for Ag,[23] and for In, Sn, and Sb,[30] which have much less effective *sp*-electron screening. Similar agreement is achieved when HF-SCF calculations, including relativistic corrections, are compared to data for Ag, Cd, In, Sn, and Sb.[8] In that work,[8] energy corrections from the Breit interaction, vacuum polarization, self-energy, and quantum-electrodynamic effects were assumed to be negligible for the $M_{4,5}M_{4,5}$ final state,[8] indicating a small influence of relativistic effects on the calculated multiplet splittings. Another puzzling feature is that, for Cd, $^1G_4$ absolute energies calculated relativistically agree better with experiment than do those calculated nonrelativistically, even though the relativistic Coulomb integrals involve a final double-hole configuration in contrast to

TABLE V. Parameters used in applying the image model discussed in the text to the $L_{2,3}M_{4,5}M_{4,5}$ of Rh and Pd (exemplified by Fig. 4). For each metal, the second column represents the calculated satellite position relative to that of the main peak from Eqs. (1) and (2). The multiplet splittings of the satellite spectra are the same as those given in Tables I and II. The images are formed by multiplying each multiplet term by a Gaussian of form $D\ \exp[-[(E-E_j)/\Gamma]^2]$, where E_j denotes the term energy, and the amplitude D and half-width Γ are the same for all terms in a multiplet. The third column for each metal represents 2Γ. The quantity L_i Int. ($i=3$ or 2) in the last two columns for each metal denotes the intensity relative to that of the atomic part, and is equal to $D\Gamma\sqrt{\pi}$.

	Rh				Pd			
	$\Delta\varepsilon$ (eV)	2Γ (eV)	L_3 Int.	L_2 Int.	$\Delta\varepsilon$ (eV)	2Γ (eV)	L_3 Int.	L_2 Int.
Atomic	0.0	3.9	1.0	1.0	0.0	3.1	1.0	1.0
Sat. 2	−1.5	8.0	0.46	0.46	−3.79	7.4	0.66	0.66
Sat. 1	−8.2	9.0	0.41	0.41	−12.1	8.9	0.32	0.32

the neutral ground state used for the nonrelativistic calculations.[8]

To add further to the puzzle, we should cite work on the $M_{4,5}N_{4,5}N_{4,5}$ transition in Cd.[44] In that case, the nonrelativistic calculations using ground-state basis functions overestimated the multiplet splitting, even though they predicted the spin-orbit coupling correctly, and it was suggested that the discrepancy might be caused by neglecting relativistic effects:[44] configuration interaction and correlation effects were eliminated as causes of the discrepancy. From these considerations, one conclusion seems to emerge: the correct choice of charge state for determining the basis functions used in the Coulomb integrals is not clear and would seem to depend on the transition involved.

Presumably, an improved relativistic calculation of the multiplet energies would produce a pattern of Rh intensities quite similar to those resulting from our calculation. It is interesting to note that Fig. 1 makes obvious the explanation of how the relativistic calculation for Rh could be used to describe an Auger spectrum of Pd.[14,16,17,19] The nonrelativistic results for Pd, illustrated in Fig. 1, agree rather well with the experimental spectra.

We should point out that the nonrelativistic calculations are probably reliable in predicting the forms of the $L_{1,2,3}M_{4,5}M_{4,5}$ Auger spectra, even for these open shell metals, since the relative intensities of the most important lines of Rh are quite close to those calculated relativistically and these relative intensities seem to vary slowly with atomic number, as we can deduce by inspecting Tables I–III. The relative simplicity of the nonrelativistic calculations would appear to make it advantageous for them to be used by nonspecialists in calculation.

Since the main theme of this paper is that of comparing the atomic portions of these experimental spectra with atomic theoretical results, we shall only briefly discuss the satellites[28] in Figs. 1–3. The similarity in form of the L_2 and $L_3M_{4,5}M_{4,5}$ satellites, and their difference from the $L_1M_{4,5}M_{4,5}$ satellite, would seem to reflect the variation of the linewidths of the initial XPS core levels; measurements[45] indicate that L_2 and L_3 levels have very similar linewidths for both Pd and Rh, which are considerably narrower than that of the L_1 level [similar systematics is observed for Ag (Ref. 29) as well]. Such a linewidth dependence is consistent with theoretical predictions.[46] It is interesting to note that the presence of the $L_1M_{4,5}M_{4,5}$ satellite, which seem to have the same origin as those of the other spectra,[31,32] emphasizes the importance of shake-up processes and would seem to deny the importance of the contributions of Coster-Kronig processes.[12]

Indicated in Figs. 1–3 by downward solid triangles are the calculated positions of the satellites if we assume the satellite closest to the main peak arises from one spectator vacancy in the $4d$ valence band and the satellite furthest from the main peak arises from two spectator vacancies,[23] and if we suppose the excited atom model[47] is applicable. In previous work,[31,32] we applied this model to experimental $L_{2,3}M_{4,5}M_{4,5}$ data, supposing that the loss peaks correspond to two well-defined spectator vacancy states, each of which is a broadened image of the main atomic spectrum characterized by the multiplet terms in Tables I and II. Application to the data[31,32] is generated from the multiplet calculations by multiplying each of the terms by a Gaussian of constant amplitude and width centered at the term position. In Fig. 4, we exemplify, for the $L_3M_{4,5}M_{4,5}$ spectrum of Pd, the results of applying this image model. In Table V, we present the relevant parameters resulting from applying this satellite image model to experimental data[31,32] for the $L_{2,3}M_{4,5}M_{4,5}$ spectra of Rh and Pd. The relative satellite positions are calculated from a model presented earlier.[23] That is, $\Delta\varepsilon(Z)$, the relative position of the one-hole satellite (i.e., satellite 2) relative to the main peak in metal of atomic number Z, is given by Eq. (1):

$$\Delta\varepsilon(Z)\cong B_l(Z+2)-B_l(Z+1), \tag{1}$$

where $B_l(Z)$ is the binding energy of level l in metal of atomic number Z. In our case, level l is the $N_{4,5}$ level, a valence d-band state. The relative position of the two-hole satellite (i.e., satellite 1), $\Delta\varepsilon_2(Z)$, is given by Eq. (2):

$$\Delta\varepsilon_2(Z)\cong B_m(Z+2)-B_m(Z+1)+\xi_{lm}(Z+2)-\xi_{lm}(Z+1), \tag{2}$$

where $\xi_{lm}(Z)$ is the Auger parameter (or effective Coulomb interaction) between the l and m holes (here, $l=m=N_{4,5}$). The binding energies and Auger parameters for Rh and Pd utilized in making Table V were taken from XPS data.[48,49]

IV. CONCLUSIONS

In this paper, we present the results of nonrelativistic calculations of the $L_{1,2,3}M_{4,5}M_{4,5}$ spectra of Pd and Rh and show that they describe, reasonably well, high-resolution spectra excited with radiation from a Ti anode. Comparison with more sophisticated calculations of the Rh spectra, including such effects as relativity and configuration interaction,[33] indicates that the nonrelativistic theoretical spectra appear to describe the Rh data better than the more sophisticated calculation. Closer inspection indicates that the relative intensities of the stronger multiplet components are very similar in both calculations; intensity differences introduced by including effects of relativity and configuration interaction would not appear to be experimentally observable. In fact, from comparing nonrelativistic Pd and Ag results, it appears that the intensities vary relatively little with atomic number. The difference between the degrees of agreement with experiment of the two calculations for Rh appears to be a result of the calculation of the multiplet splittings. Since our spin-orbit splittings are derived from XPS data and the relativistic calculations[33] yield the multiplet splittings directly, the observed discrepancies appear to derive from calculating the Slater integrals for the initial hole state in the relativistic calculations; relativistic corrections do not appear to be important in determining the multiplet splitting. In any case, it becomes clear that one could describe the data in Rh, Pd, and Ag fairly well by using relative multiplet intensities calculated for Rh, for example, for all three metals, if we include an accurate multiplet splitting for each case. This would explain how Pd Auger spectral data could be described by Rh calculations.[14,16,17,19]

All three spectra of Rh and Pd display satellites at negative relative energies. Their presence in the $L_1M_{4,5}M_{4,5}$ spectra would suggest that shake-up, rather than the Coster-Kronig process, dominates in these spectra, in contrast to previous findings.[12] Furthermore, their dependence upon the linewidth of the initial XPS state would appear to be consistent with theoretical predictions.[46] These satellites would appear to be explained by a model in which they arise from one- and two-spectator vacancies in the $4d$ valence band. Utilization of this model to calculate the satellite positions, as well as their line shapes, assuming that the satellites correspond to images of the main atomic spectrum, yields reasonable agreement with the data.[31,32] We illustrate the agreement for the $L_3M_{4,5}M_{4,5}$ of Pd.

TABLE VI. $L_1M_{4,5}M_{4,5}$ transition rates in jj-IC.

$J=0$	$25\lvert C_i(^1S_0)A(0,0)\rvert^2$
$J=2$	$625\lvert C_i(^1D_2)A(2,2)\rvert^2$
$J=4$	$2025\lvert C_i(^1G_4)A(4,4)\rvert^2$

ACKNOWLEDGMENTS

The authors would like to thank FAPESP, CNPq, and FINEP of Brazil for financial support.

APPENDIX

The general equations for Auger spectra with two equivalent final-state holes were presented earlier.[30,40] The specific equations used for calculating the transition rates appropriate for the $L_{2,3}M_{4,5}M_{4,5}$ spectra reported in this paper are those presented in Ref. 30. The $L_1M_{4,5}M_{4,5}$ transition rates are those given in Table VI. The expressions for the $A(L,l_2)$ are given in Eqs. (A1)–(A3):

$$A(0,0)=\frac{1}{\sqrt{5}}D(2,0), \tag{A1}$$

$$A(2,2)=-\tfrac{1}{5}\sqrt{\tfrac{2}{7}}D(2,2), \tag{A2}$$

$$A(4,4)=\tfrac{1}{3}\sqrt{\tfrac{2}{35}}D(2,4), \tag{A3}$$

where the radial matrix element is taken to be

$$D(k,l_2)=\frac{1}{2k+1}\int dr_1\int dr_2\phi_{2s}(r_1)\phi_{l_2}(r_2)\times\left(\frac{(r_<)^k}{(r_>)^{k+1}}\right)\phi_{4d}(r_1)\phi_{4d}(r_2), \tag{A4}$$

where the ϕ_{nl}'s are one-electron Hartree-Fock eigenfunctions and the C's used in calculating the transition rates are given in Table IV.

[1] J. C. Fuggle, in *Electron Spectroscopy*, edited by C. R. Brundle and A. D. Baker (Academic, London, 1981), p. 85.
[2] P. Weightman, Rep. Prog. Phys. **45**, 753 (1982).
[3] J. E. Houston and R. R. Rye, Comments Solid State Phys. **10**, 233 (1983).
[4] S. Lundquist and R. Schrieffer, Phys. Scr. **34**, 84 (1986).
[5] G. G. Kleiman, Appl. Surf. Sci. **11-12**, 730 (1982).
[6] E. D. Roberts, P. Weightman, and C. E. Johnson, J. Phys. C **8**, L301 (1975).
[7] E. Antonides, E. C. Janse, and G. A. Sawatzky, Phys. Rev. B **15**, 1669 (1977).
[8] P. Weightman, J. F. McGilp, and C. E. Johnson, J. Phys. C **9**, L585 (1976).
[9] J. F. McGilp and P. Weightman, J. Phys. C **9**, 3541 (1976).
[10] A. C. Parry-Jones, P. Weightman, and P. T. Andrews, J. Phys. C **12**, 1587 (1979).
[11] J.-M. Mariot and M. Ohno, Phys. Rev. B **34**, 2182 (1986).
[12] S. L. Sorensen, R. Carr, S. J. Schaphorst, S. B. Whitfield, and B. Crasemann, Phys. Rev. A **39**, 6241 (1989).
[13] W. Drube, R. Treusch, and G. Materlik, Phys. Rev. Lett. **74**, 42 (1995).
[14] W. Drube, A. Lessmann, and G. Materlik, Jpn. J. Appl. Phys., Part 1 **32**, 173 (1993).
[15] W. Drube, R. Treusch, R. Dähn, M. Griebenow, M. Grehk, and G. Materlik, J. Electron Spectrosc. Relat. Phenom. **79**, 223 (1996).
[16] W. Drube, Radiat. Phys. Chem. **51**, 335 (1998).
[17] W. Drube, T. M. Grehk, R. Treusch, and G. Materlik, J. Electron Spectrosc. Relat. Phenom. **88-91**, 683 (1998).
[18] T. M. Grehk, W. Drube, G. Materlik, J. E. Hansen, and T. K. Sham, J. Electron Spectrosc. Relat. Phenom. **88-91**, 241 (1998).

[19] T. M. Grehk, W. Drube, R. Treusch, and G. Materlik, Phys. Rev. B **57**, 6422 (1998).
[20] R. Landers, P. A. P. Nascente, S. G. C. de Castro, and G. G. Kleiman, J. Phys.: Condens. Matter **4**, 5881 (1992).
[21] R. Landers, P. A. P. Nascente, S. G. C. de Castro, and G. G. Kleiman, Surf. Sci. **287/288**, 802 (1993).
[22] G. G. Kleiman, R. Landers, and S. G. C. de Castro, J. Electron Spectrosc. Relat. Phenom. **68**, 329 (1994).
[23] G. G. Kleiman, R. Landers, and S. G. C. de Castro, Phys. Rev. B **49**, 2753 (1994).
[24] R. Landers, S. G. C. de Castro, and G. G. Kleiman, Surf. Sci. Spectra **2**, 177 (1993).
[25] R. Landers, G. G. Kleiman, and S. G. C. de Castro, J. Electron Spectrosc. Relat. Phenom. **72**, 211 (1995).
[26] George G. Kleiman, Phys. Status Solidi B **192**, 503 (1995).
[27] G. G. Kleiman, R. Landers, and S. G. C. Castro, in *Surfaces, Vacuum, and Their Applications*, edited by Isaac Hernández-Calderón and René Asomoza (AIP Press, Woodbury, NY, 1996), p. 65.
[28] R. Landers, S. G. C. de Castro, A. de Siervo, and G. G. Kleiman, J. Electron Spectrosc. Relat. Phenom. **94**, 253 (1998).
[29] R. Landers, A. Siervo, S. G. C. de Castro, and G. G. Kleiman, J. Electron Spectrosc. Relat. Phenom. **93**, 221 (1998).
[30] G. G. Kleiman, R. Landers, P. A. P. Nascente, and S. G. C. de Castro, Phys. Rev. B **46**, 1970 (1992).
[31] R. Landers, G. G. Kleiman, and S. G. C. de Castro, J. Electron Spectrosc. Relat. Phenom. **76**, 345 (1995).
[32] G. G. Kleiman, R. Landers, and S. G. C. de Castro, Surf. Sci. **357-358**, 251 (1996).
[33] M. H. Chen, Phys. Rev. A **31**, 177 (1985).
[34] C. J. Powell, N. E. Erickson, and T. Jach, J. Vac. Sci. Technol. **20**, 625 (1981).
[35] D. A. Shirley, Phys. Rev. B **5**, 4709 (1972).
[36] E. U. Condon and G. H. Shortley, *The Theory of Atomic Spectra* (Cambridge University Press, London, 1963).
[37] J. B. Mann, Los Alamos Scientific Laboratory Report No. LASL-3690, 1967 (unpublished).
[38] R. Nyholm and N. Mårtensson, J. Phys. C **13**, L279 (1980).
[39] E. J. McGuire, Sandia Laboratory Report No. SC-RR-710075, 1971 (unpublished).
[40] J. F. McGilp, P. Weightman, and E. J. McGuire, J. Phys. C **10**, 3445 (1977).
[41] A. de Siervo, R. Landers, G. G. Kleiman, S. G. C. de Castro, and J. Morais, J. Electron Spectrosc. Relat. Phenom. (to be published).
[42] J. C. Slater, *Quantum Theory of Atomic Structure* (McGraw-Hill, New York, 1960).
[43] M. H. Chen, B. Crasemann, and H. Mark, Phys. Rev. A **21**, 442 (1980).
[44] P. Weightman, J. Phys. C **9**, 1117 (1976).
[45] A. de Siervo, R. Landers, S. G. C. de Castro, and G. G. Kleiman, J. Electron Spectrosc. Relat. Phenom. **88-91**, 429 (1998).
[46] O. Gunnarsson and K. Schönhammer, Phys. Rev. B **22**, 3710 (1980).
[47] A. R. Williams and N. D. Lang, Phys. Rev. Lett. **40**, 954 (1978).
[48] N. Mårtensson and R. Nyholm, Phys. Rev. B **24**, 7121 (1981).
[49] We have taken the binding energy of the $N_{4,5}$ in Rh and Pd as equal to $\frac{1}{2}$ the uncorrelated experimental double hole binding energy from Ref. 48.